Screening length and quantum and transport mobilities of a heterojunction in the presence of the Rashba effect

W. Xu*

Department of Theoretical Physics, Research School of Physical Sciences and Engineering, Australian National University, Canberra ACT 0200, Australia and Institute of Solid State Physics, Chinese Academic of Sciences, Hefei 230031, China

(Received 6 September 2004; revised manuscript received 18 October 2004; published 3 June 2005)

A theoretical approach is developed to study the electronic and transport properties of a two-dimensional electron gas (2DEG) in the presence of spin-orbit interaction (SOI) induced by the Rashba effect. The standard random-phase approximation is employed to calculate the screening length caused by electron-electron interaction in a spin-split 2DEG. The quantum and transport mobilities in different spin branches are evaluated using the momentum-balance equation derived from a Boltzmann equation. Here the electron interactions with both the remote and background impurities are taken into account in an InAlAs/InGaAs heterojunction at low temperatures. It is found that in the presence of SOI, the screening length and quantum and transport mobilities differ in different spin branches. The interesting features of these important spintronic properties are presented and analyzed. Moreover, the theoretical results are compared with those obtained experimentally.

DOI: 10.1103/PhysRevB.71.245304 PACS number(s): 73.63.Hs, 72.15.Lh, 71.70.Ej

I. INTRODUCTION

In recent years, there has been an intensive investigation into spin-polarized electronic systems. At present, one important aspect in the field of spin electronics (or spintronics) is to study spin-orbit interaction (SOI) in narrow-gap semiconductor nanostructures in the absence of an external magnetic field B. The progress made in realizing spin-split electron gas systems at $B=0$, such as InAs-based and InGaAs-based two-dimensional electron gases (2DEGs),[1] has led to recent proposals dealing with advanced electronic devices such as spin transistors,[2] spin filters,[3] spin waveguides,[4] etc. Such devices have potential applications in future quantum computation. It is known that in narrow-gap semiconductor quantum wells, the spin splitting at $B=0$ (or spontaneous spin splitting) for carriers can be achieved by the inversion asymmetry of the microscopic confining potential due to the presence of the heterojunction.[5] This corresponds to an inhomogeneous surface electric field and, hence, is electrically equivalent to the Rashba spin splitting or Rashba effect.[6] The published experimental results[7,8] have indicated that in InAs-based and InGaAs-based 2DEG systems, the spontaneous spin splitting is mainly induced by the Rashba effect which can be enhanced further with increasing the gate voltage applied and/or changing the sample growth parameters.[9] Other contributions such as the Dresselhaus term is relatively weak, because it comes mainly from the bulk-inversion asymmetry of the material.[10]

In order to apply the spintronic systems as electronic devices such as spin-based transistors, it is fundamental to study the effect of SOI on electronic and transport properties of these device systems. Currently, one of the most popularly used experimental techniques to identify the Rashba spin splitting is magnetotransport measurements carried out at quantizing magnetic fields and low-temperatures at which the Shubnikov-de Hass (SdH) oscillations are observable.[1,8,9,11] From the periodicity of the SdH oscillations, the electron density in different spin branches, together with the Rashba parameter, can be determined experimentally. Moreover, using the amplitude of the SdH oscillations, the quantum mobility (or quantum lifetime) for electrons in different spin branches can also be obtained via famous Dingle plot.[12–14] Thus, the spintronic properties in a spin-split 2DEG, such as the electron distribution and quantum mobility in different spin orbits, are experimentally measurable. These experimental techniques are akin to those employed in the investigation of spin-degenerate 2DEGs in the presence of more than one occupied electronic subbands.[13–16] More importantly, it has been observed experimentally that in InAs-based and InGaAs-based spintronic systems, although the electron densities can differ significantly in different spin branches,[9,11] the quantum mobilities in the "$\pm$" spin orbits depend very weakly on the strength of SOI.[9] Such result is in sharp contrast to what has been seen in spin-degenerate (e.g., GaAs-based) 2DEGs with more than one occupied subbands, where both quantum and transport mobilities differ significantly in different electronic subbands. In order to understand this important and interesting experimental finding and to achieve an in-depth understanding of how SOI affects the electronic and transport properties of a 2DEG, in this paper I present a tractable theoretical approach to examine quantum and transport mobilities pertinent to a spin-split 2DEG.

Very recently, the magnetotransport properties of a spin-split 2DEG has been studied theoretically by Vasilopoulos and co-worker.[17] In their work, the effect of the Landau quantization induced by the presence of high magnetic fields has been considered and the profile of the SdH oscillations has been obtained theoretically. In this paper, I limit myself to the case where the magnetic field is absent. It is well known that although the quantum mobility is determined from experimental data obtained at $B\neq 0$, the theoretical evaluation of this transport coefficient can be simply achieved via investigating the small-angle scattering at $B=0$.[12,13,18] For case of spin-degenerate 2DEGs, the theoretical results obtained from this approach agree very well with

those obtained experimentally. In this work, I generalize this approach to study both the quantum and transport mobilities in a spin-split 2DEG. The paper is organized as follows. The one-particle aspects and the features of electron-impurity scattering in a spin-split 2DEG are briefly examined in Sec. II. In Sec. III, the effect of SOI on electron-electron interaction is investigated using a standard random-phase approximation. In Sec. IV, the quantum and transport mobilities in different spin branches are evaluated using a momentum-balance equation derived from a Boltzmann equation. The analytical results for the matrix element of electron interaction with remote and background impurities in an InGaAs/InAlAs heterojunction are presented in Sec. V. Numerical results are given and discussed in Sec. VI and the concluding remarks are summarized in Sec. VII.

II. ONE-PARTICLE ASPECTS

For a 2DEG formed in the *xy* plane in an InGaAs/InAlAs heterojunction (the growth direction is taken along the *z* axis), the effective effect of SOI can be obtained from, e.g., a $\mathbf{k}\cdot\mathbf{p}$ band structure calculation.[1,5] Including the lowest order of the SOI induced by the Rashba effect, the single-electron Hamiltonian in the absence of electronic scattering centers can be solved analytically.[4] The electron wave function and corresponding energy spectrum are given, respectively, by

$$\Psi_{\sigma\mathbf{k}n}(\mathbf{R}) = |\sigma,\mathbf{k},n\rangle = \frac{1}{\sqrt{2}}\begin{bmatrix} 1 \\ \sigma(k_y - ik_x)/k \end{bmatrix} e^{i\mathbf{k}\cdot\mathbf{r}}\psi_n(z), \quad (1)$$

and

$$E_{\sigma n}(\mathbf{k}) = E_\sigma(\mathbf{k}) + \varepsilon_n = \frac{\hbar^2 k^2}{2m^*} + \sigma\alpha k + \varepsilon_n. \quad (2)$$

Here, $\mathbf{k}=(k_x,k_y)$ is the electron wave vector along the 2D plane, $\mathbf{R}=(\mathbf{r},z)=(x,y,z)$, m^* is the electron effective mass, α is the Rashba parameter which measures the strength of the spin-orbit coupling, and $\sigma=\pm 1$ refers to different spin branches. The wave function $\psi_n(z)$ and energy ε_n for an electron in the *n*th electronic subband are determined by a spin-independent Schrödinger equation along the *z* axis, because SOI does not affect the electron states along the growth direction.

Using Eq. (2), the Green's function for a spin-split 2DEG can be obtained and the density-of-states (DOS) for such an electronic system can be determined from the imaginary part of the Green's function. In this paper, we consider a heterojunction in which only the lowest electronic subband is present (i.e., $n'=n=0$) and we measure the energy from $\varepsilon_0=0$. After using the condition of total electron number conservation, the Fermi energy E_F and electron density n_σ in the σ spin branch are obtained, respectively, for low temperatures $T\to 0$, as

$$E_F = \frac{\hbar^2}{m^*}(\pi n_e - k_\alpha^2), \quad (3)$$

and

$$n_\sigma = \frac{n_e}{2} - \sigma\frac{k_\alpha}{2\pi}\sqrt{2\pi n_e - k_\alpha^2}. \quad (4)$$

Here $n_e=n_-+n_+$ is the total electron density and $k_\alpha = m^*\alpha/\hbar^2$. In low energy regime where is most possibly occupied by electrons, the DOS for the "$-$" branch is always larger than that for the "$+$" branch, and this is the main reason why electron density in spin-down channel is always larger than that in spin-up channel. The dependence of electron distribution in different spin branches on α and n_e has been presented in Ref. 19. It should be noted that with increasing α and/or decreasing n_e, Fermi energy decreases [see Eq. (3)] and, consequently, more and more electrons are in the spin-down orbit. Therefore, in a spin-split 2DEG spin polarization increases with increasing Rashba parameter and/or with decreasing total electron density, in line with experimental findings.[8,9,11]

At low-temperatures, electron-impurity (*e*-*i*) scattering is the principal channel for the relaxation of electrons in semiconductor-based 2DEG systems. The features of *e*-*i* scattering in a spin-split 2DEG have been examined recently by Huang *et al.*[20] In this section, I present a simple way to obtain the matrix element for *e*-*i* interaction in conjunction with the further calculations of the transport coefficients for a spin-split 2DEG. Applying the electron wavefunction given by Eq. (1) to the standard approach documented in, e.g., Ref. 21, the matrix element for *e*-*i* interaction induced by the Coulomb potential is obtained, in the absence of electron-electron (*e*-*e*) screening, as

$$U^0_{\sigma'\sigma}(q,\mathbf{R}_a) = \frac{2\pi Ze^2}{\kappa q}\sqrt{n_i(z_a)}F_0(q,z_a)h_{\sigma'\sigma}(\theta)e^{-i\mathbf{q}\cdot\mathbf{r}_a}\delta_{\mathbf{k}',\mathbf{k}+\mathbf{q}}. \quad (5)$$

Here, the impurity is located at $\mathbf{R}_a=(\mathbf{r}_a,z_a)=(x_a,y_a,z_a)$, Z is its charge number, κ is the static dielectric constant of the material, $\mathbf{q}=(q_x,q_y)$ is the Fourier transform factor which corresponds to the change of electron wave vector during an *e*-*i* scattering event, and $n_i(z_a)$ is the impurity distribution along the growth direction. Furthermore, $F_0(q,z_a) = \int dz|\psi_0(z)|^2 e^{-q|z-z_a|}$ is the form factor for *e*-*i* scattering in a 2D system and $h_{\sigma'\sigma}(\theta)=[1+\sigma'\sigma(\cos\theta - i\sin\theta)]/2$ is a spin-dependent matrix element with θ being the angle between $\mathbf{k}'$ and $\mathbf{k}$. From Eq. (5), we see that similar to a spin-degenerate 2DEG, the electron-impurity interaction matrix element diverges in a spin-split 2DEG when $q\to 0$. Hence, it is necessary to include the effect of *e*-*e* screening on electron-impurity scattering when calculating the transport coefficients.

III. DIELECTRIC FUNCTION AND SCREENING LENGTH

We now study many-body effects of a 2DEG in the presence of SOI. Although this topic was noticed by Chen *et al.*,[22] most of the results presented in Ref. 22 were obtained for small q limit (i.e., $q \ll k_F$) and were for screened interaction potential. In this section, we focus on screening length induced by *e*-*e* interaction, which can be used for further calculations in the later part of the paper. Applying the elec-

tron wave function given by Eq. (1) to the *e-e* interaction Hamiltonian induced by the Coulomb potential, the space Fourier transform of the matrix element for bare *e-e* interaction can be determined. From the electron energy spectrum given by Eq. (2), one can derive the retarded and advanced Green functions for electrons when the effect of SOI is taken into consideration. Applying these Green functions along with the bare *e-e* interaction to the diagrammatic techniques to derive effective *e-e* interaction under the random-phase approximation (RPA), one can determine first the effective *e-e* interaction and then the dynamical dielectric function matrix, which reads[19]

$$\epsilon(\Omega,q)=\begin{bmatrix}1+a_1 & 0 & 0 & a_4\\ 0 & 1+a_2 & a_3 & 0\\ 0 & a_2 & 1+a_3 & 0\\ a_1 & 0 & 0 & 1+a_4\end{bmatrix}. \tag{6}$$

Here, the indexes $1=(++)$, $2=(+-)$, $3=(-+)$, and $4=(--)$ are defined regarding to different transition events from spin branch σ' to spin branch σ, $a_j=a_j(q)=-V_qG_0(q)\Pi_j(\Omega,q)$ with

$$V_q=2\pi e^2/\kappa q$$

and

$$G_0(q)=\int dz_1\int dz_2|\psi_0(z_1)|^2|\psi_0(z_2)|^2e^{-q|z_1-z_2|},$$

and

$$\Pi_{\sigma'\sigma}(\Omega,q)=\frac{1}{2}\sum_{\mathbf{k}}(1+\sigma'\sigma A_{\mathbf{kq}})\frac{f[E_{\sigma'}(\mathbf{k}+\mathbf{q})]-f[E_{\sigma}(\mathbf{k})]}{\hbar\Omega+E_{\sigma'}(\mathbf{k}+\mathbf{q})-E_{\sigma}(\mathbf{k})+i\delta}$$

is the pair bubble or density-density correlation function in the absence of *e-e* interaction.[22,23] Furthermore, $f(x)$ is the Fermi-Dirac function, an infinitesimal quantity $i\delta$ has been introduced to make the integral converge when Fourier transforming from time representation to spectrum-representation, $A_{\mathbf{kq}}=(k+q\cos\psi)/|\mathbf{k}+\mathbf{q}|$, and ψ is an angle between $\mathbf{k}$ and $\mathbf{q}$. Thus, the inverse dielectric function matrix for a spin-split 2DEG is

$$\epsilon^{-1}(\Omega,q)=\begin{bmatrix}1-a_1^* & 0 & 0 & -a_4^*\\ 0 & 1-a_2^* & -a_3^* & 0\\ 0 & -a_2^* & 1-a_3^* & 0\\ -a_1^* & 0 & 0 & 1-a_4^*\end{bmatrix}, \tag{7}$$

with $a_1^*=a_1/(1+a_1+a_4)$, $a_2^*=a_2/(1+a_2+a_3)$, $a_3^*=a_3/(1+a_2+a_3)$, and $a_4^*=a_4/(1+a_1+a_4)$. It should be noted that in contrast to Eq. (15) in Ref. 22, here I use a matrix to present the dielectric function $\epsilon(\Omega,q)$. For a spin-split 2DEG which is also a two-level system when only the lowest subband is included, there are four channels for electronic transitions (i.e., $j=1$, 2, 3, and 4 defined here) induced by *e-e* interaction. From the fact that a transition event j should be affected by other transition events due to *e-e* interaction, the dielectric function for a spin-split 2DEG (i.e., for a two-level system) is therefore a 4×4 matrix. Moreover, $j=1$ and 4 (2 and 3) here correspond to intra-SO (inter-SO) transition events.

With the inverse dielectric function matrix, we can calculate the matrix element for *e-i* interaction in the presence of *e-e* screening, through the definition $U_i(q,\mathbf{R}_a)=\Sigma_jU_i^0(q,\mathbf{R}_a)\epsilon_{ij}^{-1}(q)$. Here $\epsilon_{ij}(q)=\epsilon_{ij}(\Omega\to0,q)$ is the element of static dielectric function matrix. Using Eq. (5), the square of the matrix element for electron-impurity interaction in the presence of *e-e* screening becomes

$$|U_1(q,\theta)|^2=|U_4(q,\theta)|^2=|U_+(q,\theta)|^2\delta_{\mathbf{k}',\mathbf{k}+\mathbf{q}} \tag{8}$$

for intra-SO scattering, and

$$|U_2(q,\theta)|^2=|U_3(q,\theta)|^2=|U_-(q,\theta)|^2\delta_{\mathbf{k}',\mathbf{k}+\mathbf{q}} \tag{9}$$

for inter-SO scattering. Here,

$$|U_\pm(q,\theta)|^2=\left(\frac{2\pi Ze^2}{\kappa}\right)^2\frac{h_\pm(\theta)}{[q+K_\pm(q)]^2}\int dz_an_i(z_a)F_0^2(q,z_a), \tag{10}$$

$h_\pm(\theta)=(1\pm\cos\theta)/2$ and the inverse screening length for intra-SO $[K_+(q)]$ and inter-SO $[K_-(q)]$ transitions is obtained, at $T\to0$, as

$$K_\pm(q)=\frac{16e^2m^*}{\pi\hbar^2\kappa q}G_0(q)\sum_\sigma\int_0^{\sqrt{4\pi n_\sigma}}dk\times\frac{k(k+q)}{(2k+q+2\sigma k_\alpha)(k+q+|k-q|)}H_\sigma^\pm(k,q), \tag{11}$$

where

$$H_\sigma^\pm(k,q)=\frac{-1\pm1}{2}K(\mathcal{A})+\Pi(\mathcal{AB}_\pm,\mathcal{A})+\frac{q(q+2\sigma k_\alpha)}{4k(k+\sigma k_\alpha)}[\Pi(\mathcal{AC}_\pm,\mathcal{A})-\Pi(\mathcal{AB}_\pm,\mathcal{A})], \tag{12}$$

$K(x)$ is the complete elliptic integral of the first kind, $\Pi(n,x)=\Pi(\pi/2,n,x)$ is the complete elliptic integral of the third kind, $\mathcal{A}=(k+q-|k-q|)/(k+q+|k-q|)$, $\mathcal{B}_\pm=[(2k+q)/q]^{\pm1}$, and $\mathcal{C}_\pm=[(q-2\sigma k_\alpha)/(2k+q+2\sigma k_\alpha)]^{\pm1}$. It implies that in the presence of SOI, the intra-SO and inter-SO transitions have different screening lengths. The results shown above are obtained without assuming $q\ll k_F$, in contrast to those obtained by Ref. 22.

IV. SPIN-DEPENDENT QUANTUM AND TRANSPORT MOBILITIES

Although transport equations for spin-split 2DEGs have been proposed very recently,[23] the actual calculations of the transport coefficients for these systems have not been well documented. In this section, I present a simple approach to examine quantum and transport mobilities of a 2DEG in the presence of SOI. From the above presented results and using the Fermi's golden rule, the electronic transition rate induced by *e-i* scattering is obtained as

$$W_{\sigma'\sigma}(\mathbf{k}',\mathbf{k}) = \frac{2\pi}{\hbar}|U_{\sigma'\sigma}(q,\theta)|^2\delta_{\mathbf{k}',\mathbf{k}+\mathbf{q}}\delta[E_{\sigma'}(\mathbf{k}') - E_{\sigma}(\mathbf{k})]. \tag{13}$$

We now consider a weak dc electric field F_x applied along the 2D plane (taken along the x direction) of a spin-split 2DEG. In the steady state the corresponding semiclassical Boltzmann equation, for nondegenerate statistics, reads

$$-\frac{eF_x}{\hbar}\frac{\partial f_\sigma(\mathbf{k})}{\partial k_x} = \sum_{\mathbf{k}',\sigma'}[f_{\sigma'}(\mathbf{k}')W_{\sigma\sigma'}(\mathbf{k},\mathbf{k}') - f_\sigma(\mathbf{k})W_{\sigma'\sigma}(\mathbf{k}',\mathbf{k})], \tag{14}$$

where $f_\sigma(\mathbf{k})$ is the momentum-distribution function for an electron at a state $|\sigma,\mathbf{k}\rangle$. We assume that $f_\sigma(\mathbf{k}) = f[E_\sigma(\mathbf{k} - m^*\mathbf{v}_\sigma/\hbar)]$ can be described by the drifted energy distribution function. Here $\mathbf{v}_\sigma = v_\sigma(1,0,0)$ is the average drift velocity of an electron in the σ spin branch along the x direction due to the presence of F_x. For the first moment, the momentum-balance equation[24] can be derived by multiplying k_x to both sides of the Boltzmann equation and by summing over $\mathbf{k}$. For a weak driving field F_x so that $v_\sigma \ll \hbar k_x/m^*$ and $f_\sigma(\mathbf{k}) \simeq f[E_\sigma(k)] - \hbar k_x v_\sigma(1+\sigma k_\alpha/k)\, f'(E)|_{E=E_\sigma(k)}$ with $f'(E) = \partial f(E)/\partial E$, the momentum-balance equation gives

$$1 = \sum_{\sigma'}[\mu_t^\sigma B_{\sigma'\sigma} - \mu_t^{\sigma'} C_{\sigma\sigma'}]. \tag{15}$$

Here $\mu_t^\sigma = -v_\sigma/F_x$ is the *transport* mobility for an electron in spin branch σ and

$$(B_{\sigma'\sigma}, C_{\sigma'\sigma}) = -\frac{\hbar^2}{e}\sum_{\mathbf{k}',\mathbf{k}}\left(\frac{k_x}{n_\sigma}, \frac{k'_x}{n_{\sigma'}}\right)k_x(1+\sigma k_\alpha/k) \times W_{\sigma'\sigma}(\mathbf{k}',\mathbf{k})f'(E)|_{E=E_\sigma(k)}. \tag{16}$$

It can be seen that the term $B_{\sigma'\sigma}$ is induced by small-angle scattering between $\mathbf{k}'$ and $\mathbf{k}$. Hence, by definition,[12,18,25] the *quantum* mobility for electrons in spin branch σ, μ_q^σ, is given by

$$\frac{1}{\mu_q^\sigma} = \sum_{\sigma'} B_{\sigma'\sigma}. \tag{17}$$

The transport mobility, μ_t^σ, in different spin branches can be determined by solving Eq. (15) and the average transport mobility is given as

$$\mu_t = \frac{n_+\mu_t^+ + n_-\mu_t^-}{n_e}. \tag{18}$$

As has been pointed out,[12,25] the basic differences between quantum and transport mobilities for an electronic system are (i) experimentally, the quantum mobility is determined from the amplitudes of SdH oscillations via the Dingle plot,[12–14,25] whereas the transport mobility is measured in a conventional experiment (i.e., by applying a current and measuring the voltage directly) and (ii) theoretically, the quantum mobility is induced by small-angle scattering events whereas the transport mobility includes contributions from scattering with all angles.

Using Eq. (13) for e-i scattering, we obtain, at low-temperatures (i.e., $T \to 0$)

$$(B_{\sigma'\sigma}, C_{\sigma'\sigma}) = A\int_0^\pi d\theta(\sqrt{n_{\sigma'}}, \sqrt{n_\sigma}\cos\theta)|U_{\sigma'\sigma}(q,\theta)|^2, \tag{19}$$

where $A = (m^{*2}/\pi\hbar^2 e)[4\pi/(2\pi n_e - k_\alpha^2)]^{1/2}$ and $q = [4\pi(n_{\sigma'} + n_\sigma - 2\sqrt{n_{\sigma'}n_\sigma}\cos\theta)]^{1/2}$. These results indicate that corresponding to different electronic transition channels due to e-i scattering, the change of the electron wave vector or momentum q is different. (1) For intra-SO scattering within the $+$ spin branch, $q = 4\sqrt{\pi n_+}\sin(\theta/2) = [0, 4\sqrt{\pi n_+}]$. (2) For intra-SO scattering within the $-$ branch, $q = 4\sqrt{\pi n_-}\sin(\theta/2) = [0, 4\sqrt{\pi n_-}]$. Hence, intra-SO transitions induced by e-i scattering correspond to different q factors and q can be zero at $\theta = 0$. (3) Whereas for inter-SO scattering, $q = 2\sqrt{\pi n_e - (\pi n_e - k_\alpha^2)\cos\theta} = [2k_\alpha, 2\sqrt{2\pi n_e - k_\alpha^2}]$ is the same for both a transition from the $+$ spin branch to the $-$ branch and a transition from the $-$ branch to the $+$ branch. Moreover, for inter-SO scattering, $q \neq 0$ which implies that inter-SO transition can only be achieved via varying the wave vector (or momentum) of an electron, because the spin-splitting depends explicitly on electron wave vector. Hence, in general the small-q results obtained by Ref. 22 may not be used for screened e-i scattering induced by inter-SO transitions.

V. InGaAs/InAlAs HETEROJUNCTION

In an InGaAs/InAlAs heterojunction, the impurity scattering comes mainly from: (i) ionized remote impurities within a narrow space charge layer in the InAlAs region with a concentration N_r at a spacer distance s from the interface, because of modulation doping; and (ii) charged background impurities with a depletion charge density N_{depl} and a depletion length d in the InGaAs layer, due to the effect of depletion. In general, these impurity distributions along the growth direction are not well known. In conjunction with a typical spintronic device realized from an InGaAs/InAlAs heterojunction,[7] in this paper I model the remote and background impurity distributions, respectively, as

$$n_r(z_a) = N_r\delta(z_a + s) \quad \text{and} \quad n_b(z_a) = (N_{\text{depl}}/d)\Theta(z_a). \tag{20}$$

These assumptions are mainly based on the fact that the width of the charge layer for modulation doping is relatively narrow and the depletion length in the InGaAs layer is much longer than the effective thickness of the confining potential for electrons.

For a heterojunction, we can apply the usual triangular well approximation to model the confining potential normal to the heterointerface and use the corresponding variational wavefunction for $\psi_0(z)$.[21] Thus, the square of the e-i interaction matrix element induced by scattering with remote and background impurities is given by

$$|U_{\pm}^{i}(q,\theta)|^2 = \left(\frac{2\pi Ze^2}{\kappa}\right)^2 \frac{h_{\pm}(\theta)}{[q+K_{\pm}(q)]^2} g_i(q). \qquad (21)$$

For remote impurity scattering ($i=r$), $g_r(q)=N_r e^{-2qs}/(x+1)^6$, $x=q/b$, and $b=[(48\pi m^* e^2/\kappa\hbar^2)(N_{\rm depl}+11n_e/32)]^{1/3}$. For background impurity scattering ($i=b$), $g_b(q)=N_b(3x^5+18x^4+43x^3+48x^2+24x+2)/[4x(x+1)^6]$ and $N_b=N_{\rm depl}/(db)$. We see that similar to a spin-degenerate 2DEG, electrons in a heterojunction interact more strongly with background impurities than with remote ones, especially when $q\to 0$. This is mainly due to the fact that background impurities are located in the layer where the majority of conducting electrons are. The form factor for *e-e* interaction is $G_0(q)=(3x^2+9x+8)/[8(x+1)^3]$.

It should be noted that in Ref. 17, the *e-i* scattering was accounted only for background impurities and the influence of the penetration of the wave function along the growth direction on the interaction matrix was neglected. Therefore, the present consideration of the *e-i* scattering in this paper is closer to the experimental situation of a working sample.

VI. NUMERICAL RESULTS AND DISCUSSIONS

The results of this section pertain to InGaAs/InAlAs heterojunctions at low-temperatures (i.e., $T\to 0$). The material parameters corresponding to InGaAs are taken as follows: (i) electron effective-mass $m^*=0.042m_e$ with m_e being the rest mass of an electron; (ii) static dielectric constant $\kappa=12.9$; and (iii) the typical depletion charge density $N_{\rm depl}=2\times 10^{10}$ cm^{-2}. In the calculations, we take the charge number of an impurity to be $Z=1$.

A. Screening length

From the results presented in Sec. IV, we know that for *e-i* scattering at low temperatures, the change of electron wave vector or momentum q differs for different transition channels. Thus, in order to study the effect of *e-e* interaction on transport coefficients, it is convenient to look into the angular dependence of the screen length for different transition channels. In Fig. 1, the inverse screening length $K_{\pm}(q)$ is shown as a function of θ (an angle between the initial wave vector $\mathbf{k}$ and the final wave vector $\mathbf{k}'$ during a scattering event) at a fixed total electron density n_e and a fixed Rashba parameter α. From these results, we note that: (i) $|K_{\pm}(q)|$ decreases with increasing θ, which implies that a strong effect of *e-e* screening can be achieved at small scattering angles; (ii) for intra-SO transition within the + or − spin branch, $K_+(q)\to+\infty$ when $\theta\to 0$ (i.e., $q\to 0$); (iii) $K_-(q)$ for inter-SO transition is negative and finite when $\theta=[0,\pi]$; (iv) at a fixed θ angle, $K_+(q_1)$ for transition within the + branch is always larger than $K_+(q_4)$ for transition with the − branch; and (v) at a fixed θ, the inverse screening lengths induced by intra-SO transitions, $K_+(q_1)$ and $K_+(q_4)$, are much larger than $|K_-(q_-)|$ induced by inter-SO transition. Moreover, it should be noted that at a fixed θ angle, because the transition from the − spin branch to the + spin branch corresponds to the same q as for the transition from the + branch to the − branch, the screening length is the same for inter-SO transition channels.

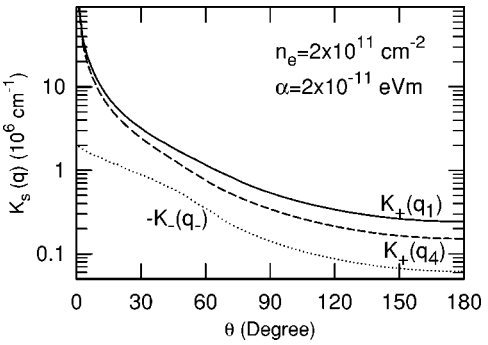

FIG. 1. Inverse screening length $K_s(q)$, $s=\pm$, for transition within the $\pm$ spin branch as a function of angle θ at a fixed total electron density n_e and a fixed Rashba parameter α. Here, θ is an angle between the initial electronic wave vector (or momentum) $\mathbf{k}$ and the final wave vector $\mathbf{k}'$, $q_1=4\sqrt{\pi n_+}\sin(\theta/2)$ for transition within the + branch, $q_4=4\sqrt{\pi n_-}\sin(\theta/2)$ for transition within the − branch, $q_-=2\sqrt{\pi n_e-(\pi n_e-k_\alpha^2)}\cos\theta$ for inter-SO transition, and $n_\pm$ is the electron density in the $\pm$ spin branch. Note that $K_-(q_-)$ is negative.

The influence of the strength of SOI and total electron density on angular dependence of the inverse screening length is shown in Figs. 2 and 3, respectively, for transition within the + and − spin channels. These results indicated that for intra-SO transitions, $K_+(q)$ increases with increasing α or with decreasing n_e. An important conclusion we can draw is that the inclusion of SOI can enhance the effect of *e-e* screening in a 2DEG for intra-SO transitions. We note that $K_+(q_1)$ (induced by transition within the + branch) depends more strongly on α and n_e than $K_+(q_4)$ (by transition

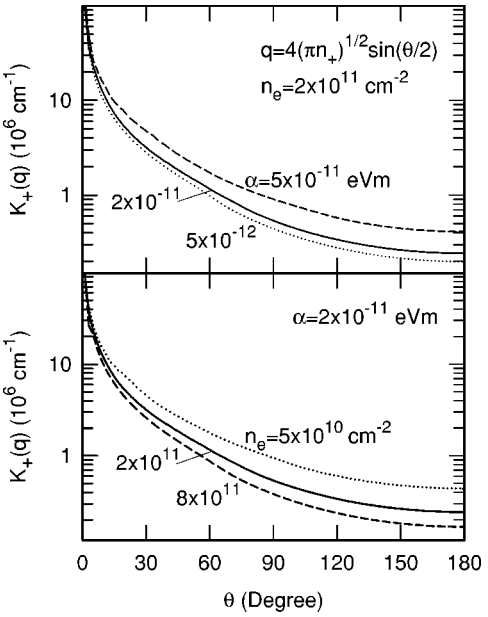

FIG. 2. Angular dependence of inverse screening length $K_+(q)$ for transition within the + spin branch. The results are shown at a fixed total electron density n_e for different Rashba parameters α (upper panel) and at a fixed α for different n_e (lower panel).

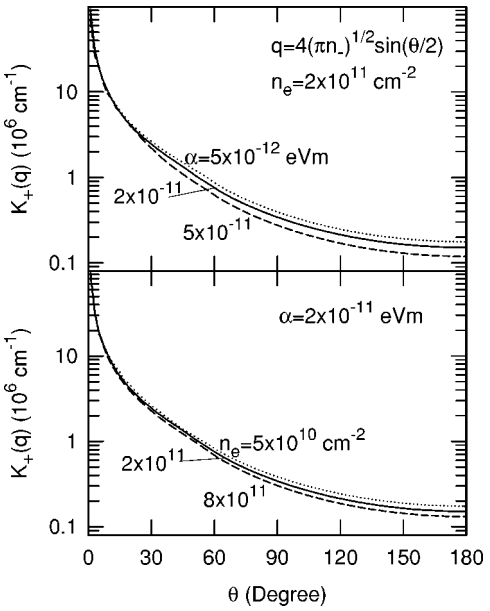

FIG. 3. Inverse screening length $K_+(q)$ for transition within the $-$ spin branch as a function of angle θ. In upper (lower) panel, the results are shown at a fixed total electron density n_e for different Rashba parameters α (at a fixed α for different n_e).

within the $-$ branch) does. The dependence of the inverse screening length induced by inter-SO transition on the Rashba parameter and total electron density is shown in Fig. 4. We see that in small θ angle regime $-K_-(q)$ increases with decreasing α or increasing n_e, whereas at large θ angles $K_-(q)$ increases with increasing α or decreasing n_e. Thus, for inter-SO transitions, the SOI can reduce the effect of *e-e* screening in the small angle regime and enhance the screening effect at the large θ angles.

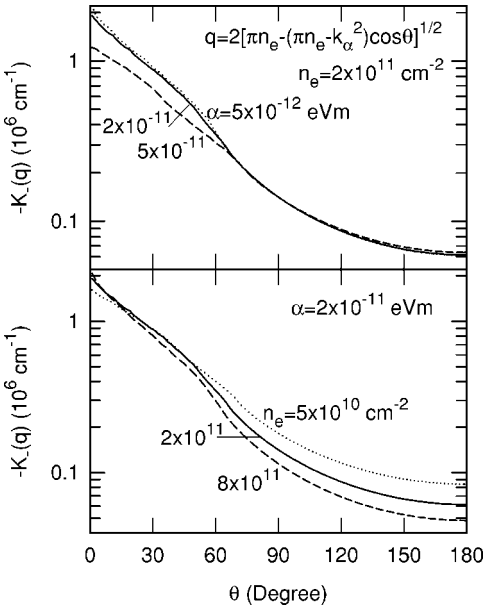

FIG. 4. Angular dependence of the inverse screening length for inter-SO transition. Note that $K_-(q)<0$ and $K_-(q)$ is the same for both inter-SO transition channels. The upper (lower) panel shows the results at a fixed total electron density (Rashba parameter) for different Rashba parameters (total electron densities).

The results shown in Figs. 1–4 indicate that in the presence of SOI, the screening length of a 2DEG differs significantly for different electronic transition channels. In particular, the *e-e* screening affects more strongly the intra-SO transitions. The main physical reason behind this important effect is that the inter-SO transition due to *e-e* interaction requires the change of the electron wave vector or momentum, because, again, the spin splitting depends explicitly on the electron wave vector. Furthermore, over a wide regime of θ or q, $|K_\pm(q)| \sim 10^5 - 10^6$ cm^{-1}, similar to the inverse screening length for a spin-degenerate 2DEG.[21]

It should be noted that in Ref. 17, the inverse screening length was taken as an input parameter and as the same for all q's and all transition channels. In the present study, $K_\pm(q)$ has been evaluated using a standard RPA approach. As can been seen, the assumption of a constant screening wave vector for different transition channels may not be the case.

B. Quantum and transport mobilities

Here we study the quantum and transport mobilities in different spin branches due to electron interactions with remote and background impurities in an InGaAs/InAlAs heterojunction. Although the concentrations N_r and N_b for remote and background impurities are normally not known, one may assume that $N_r \sim n_e$ and $N_r \gg N_b$. The former assumption is based on the fact that the conducting electrons in the InGaAs layer come mainly from ionized donors which are modulation doped in the InAlAs layer. The later assumption is made for the case of a high quality sample in which the background impurity concentration in the InGaAs layer is low. From the results presented in Secs. IV and V, we know that the square of the matrix element for electron-impurity scattering via inter-SO transition is not divergent over all defined regime of q or θ. Together with the fact that the *e-e* screening affects relatively weakly the inter-SO transition (see Figs. 1–4), in the present study we only include the effect of *e-e* screening for intra-SO transition induced by *e-i* scattering.

The dependence of the quantum and transport mobilities in different spin branches, μ_q^σ and μ_t^σ, on the Rashba parameter α is presented in Fig. 5 for the fixed n_e (total electron density), N_r and N_b (remote and background impurity concentration), and s (spacer thickness). We see that over a wide range of α, the differences between μ_q^+ and μ_q^- and between μ_t^+ and μ_t^- are relatively small, in contrast to electron distribution shown in Ref. 19. A pronounced difference between μ_q^+ and μ_q^- and between μ_t^+ and μ_t^- can only be observed at relatively large α. It can be seen that the difference between μ_t^+ and μ_t^- depends more strongly on α than that between μ_q^+ and μ_q^- does, especially at large values of α. At a large value of α, most of electrons are in the $-$ spin branch and, consequently, the average transport mobility $\mu_t \to \mu_t^-$. It is interesting to note that similar to a spin-degenerate 2DEG,[25] the transport mobility μ_t is much larger (about five times) than the quantum mobility $\mu_q^\pm$ in a spin-split 2DEG. Again, similar to a spin-degenerate 2DEG with more than one occupied

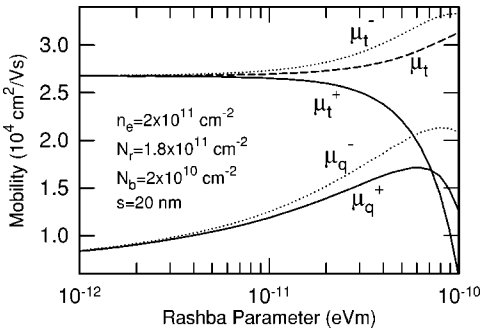

FIG. 5. Quantum and transport mobilities, $\mu_q^{\pm}$ and $\mu_t^{\pm}$, as a function of the Rashba parameter for the fixed total electron density (n_e), remote and background impurity concentration (N_r and N_b), and spacer distance (s). Here μ_t is the average transport mobility [see Eq. (18)].

electronic subbands, where larger transport mobilities have been found in lower electronic subbands,[12] a larger transport mobility can be observed at a lower energy level, here the $-$ spin branch in a 2DEG with SOI.

The physical reason behind a rather small difference of the quantum mobilities in different spin branches is the following. In contrast to a spin-degenerate 2DEG with more than one and fully quantized occupied subbands, the strength of the SOI and the energy separation of the $\pm$ branches in a spin-split 2DEG depend heavily on the electron wave vector **k**. Because the quantum mobility measures the strength of small-angle scattering, elastic and small-angle scattering implies a small momentum exchange between the two spin branches during a scattering event. As a result, the difference in the quantum mobilities between the two spin branches is relatively small in comparison to that in the transport mobilities. Roughly the same quantum mobility in different spin branches have been observed experimentally in InGaAs-based 2DEG systems.[9] The results shown in Fig. 5 suggest that a much larger α is required in order to see a significant difference between μ_q^+ and μ_q^-.

The dependence of μ_q^{σ} and μ_t^{σ} on α is shown in Fig. 6 at a fixed remote impurity concentration N_r for different background impurity concentrations N_b. We see that although N_b used here is much smaller than N_r, N_b affects strongly the value of the quantum and transport mobilities. This feature is in line with that observed in a spin-degenerate 2DEG. It can be found from Fig. 6 that with increasing the strength of the background impurity scattering (i.e., increasing N_b), the difference between μ_q^+ and μ_q^- and even between μ_t^+ and μ_t^- can become smaller. This is mainly due to the fact that electrons in a heterojunction interact more strongly with background impurities, especially for small-angle (or small q) scattering, as has been shown in Sec. V. These results confirm further that small-angle scattering in a spin split 2DEG can reduce the difference between μ_q^+ and μ_q^-.

The dependence of $\mu_q^{\pm}$ and $\mu_t^{\pm}$ on total electron density n_e is shown in Fig. 7 at a fixed remote impurity density N_r for different background impurity concentrations N_b. At high electron densities the difference between μ_q^+ and μ_q^- and between μ_t^+ and μ_t^- is suppressed because of a small difference in the electron distribution (see Ref. 19). A significant difference between μ_q^+ and μ_q^- and between μ_t^+ and μ_t^- can be seen at low electron densities. The quantum and transport mobilities increase rapidly with increasing total electron density, similar to a spin-degenerate 2DEG. Again, these mobilities depend strongly on the strength of the background impurity scattering although its concentration is relatively low. At

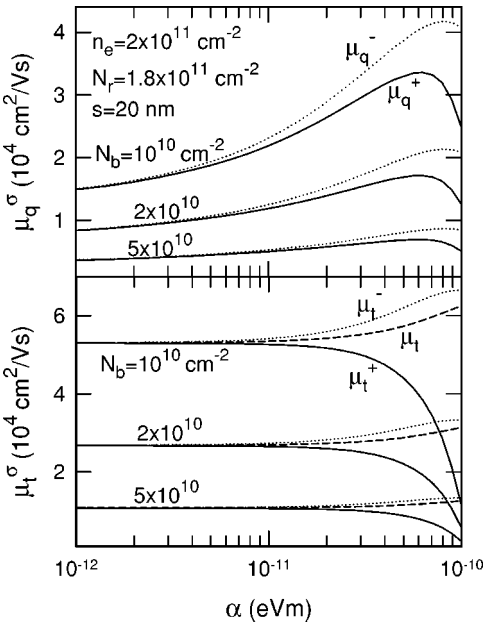

FIG. 6. Quantum and transport mobilities ($\mu_q^{\pm}$ and $\mu_t^{\pm}$ in the upper and lower panel) in different spin branches as a function of the Rashba parameter α at a fixed remote impurity concentration N_r for different background impurity concentrations N_b. Here, n_e is the total electron density and s is the spacer distance.

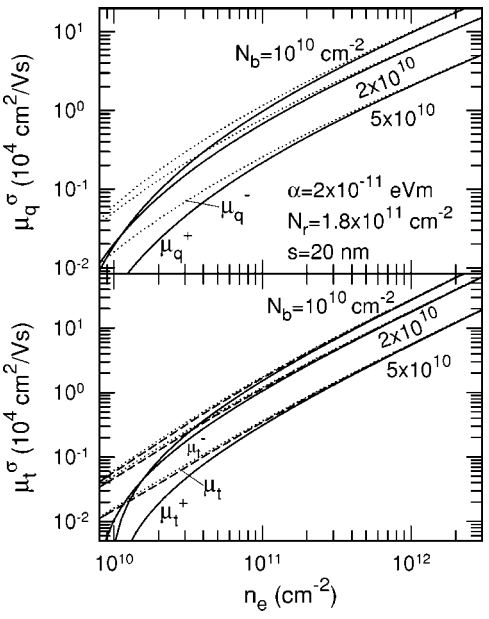

FIG. 7. Quantum and transport mobilities ($\mu_q^{\pm}$ and $\mu_t^{\pm}$ in the upper and lower panel) in different spin branches as a function of total electron density n_e at a fixed remote impurity concentration N_r for different background impurity concentrations N_b. Here, α is the Rashba parameter and s is the spacer distance.

relatively larger α and/or smaller n_e, the average transport mobility is mainly determined by electronic transition occurring at the $-$ spin branch because of the larger electron density there. Moreover, the numerical results presented here indicate that when $n_e \sim 10^{11}-10^{12}$ cm^{-2}, the transport mobility $\mu_t \sim 10^4-10^5$ cm^2/V s if $N_r \sim n_e$ and $N_b \ll N_r$ are taken into consideration. This is in line with experimental findings.[1,7,8]

One important conclusion drawn from this study is that in spintronic systems such as InGaAs/InAlAs heterojunctions in which the SOI is induced by the Rashba effect, small-angle scattering induced by *e-i* interaction cannot alter significantly the spin orientation of the electrons. To achieve a large exchange of the spin orientation in different spin branches through electronic scattering in these systems, inelastic and/or large-angle electronic transitions have to be involved. This result is useful in designing spintronic devices. At present, there are no simple experimental techniques to measure the transport mobility or lifetime in different energy levels of an electronic system. However, recently developed ultrafast optoelectronic techniques, such as femtosecond pump-and-probe experiments, have been used to determine lifetimes of electrons in different subbands in quantum well structures.[26] Although the lifetimes obtained from ultrafast pump-and-probe experiments are not exactly the same as the transport lifetimes (or mobilit) discussed in this paper, they are closely related and are of the same order of magnitude. The results shown in this paper indicate that electronic transport lifetimes in different spin branches differ significantly at large Rashba parameters or small electron densities; this implies that they may be measured by, e.g., femtosecond pump-and-probe experiments.

VII. CONCLUDING REMARKS

In this work, I have developed a tractable theoretical approach in dealing with electron-electron interaction and transport in 2DEG systems in the presence of SOI induced by the Rashba effect. The important theoretical results obtained from this study are summarized as follows.

A stronger effect of SOI on *e-e* screening and quantum and transport mobilities in different spin branches can be achieved in a device system with larger Rashba parameter and/or lower total electron density. Over a wide range of the sample parameters such as n_e and α, the quantum mobilities for electrons in both $\pm$ spin branches do not differ significantly, in line with experimental findings. This effect can be observed for electron interactions with remote and background impurities in an InGaAs/InAlAs heterojunction. The main reason behind this interesting phenomenon is that for elastic *e-i* scattering, the quantum mobility is determined by electronic transitions involving small-angle scattering or small momentum exchange. Thus, small-angle scattering induced by *e-i* interaction does not change significantly the spin transition of electrons in different spin branches.

Because transport mobility is determined by all possible electronic transition channels including large-angle scattering events, the contribution from the exchange of spin orientation in different spin branches can result in a rather significant difference in the transport mobilities in different spin branches. The theoretical results have shown that when $N_r \sim n_e$ and $N_r \gg N_b$ are taken into account, the obtained value of the average transport mobility is in line with the experimental data and the quantum and transport mobilities depend strongly on background impurity concentration N_b. It has found that the screening length and the quantum and transport mobilities in different spin branches differ significantly for *strong* values of α. Recent experimental results have shown that in InAs-based and InGaAs-based spintronic systems, the Rashba parameter can reach up to $\alpha \sim 3-4\times10^{-11}$ eV m.[1,7] The calculations in this paper have been carried out using these typical sample parameters. I therefore expect that the theoretical predictions in this paper will be tested experimentally.

ACKNOWLEDGMENTS

This work was supported by the Australian Research Council and Chinese Academy of Sciences. Discussions with P. Vasilopoulos (Concordia, Canada) are gratefully acknowledged.

*Electronic address: wen105@rsphysse.anu.edu.au

[1] D. Grundler, Phys. Rev. Lett. **84**, 6074 (2000), and references therein.

[2] B. Datta and S. Das, Appl. Phys. Lett. **56**, 665 (1990).

[3] T. Koga, J. Nitta, H. Takayanagi, and S. Datta, Phys. Rev. Lett. **88**, 126601 (2002).

[4] X. F. Wang, P. Vasilopoulos, and F. M. Peeters, Phys. Rev. B **65**, 165217 (2002).

[5] Th. Schäpers, G. Engels, J. Lange, Th. Klocke, M. Hollfelder, and H. Lüth, J. Appl. Phys. **83**, 4324 (1998).

[6] E. I. Rashba, Sov. Phys. Solid State **2**, 1109 (1960); E. I. Rashba and V. I. Sheka, in *Landau Level Spectroscopy* edited by G. Landwehr and E. I. Rashba (North-Holland, Amsterdam, 1991), Vol. 1, p. 131.

[7] Y. Sato, T. Kita, S. Gozu, and S. Yamada, J. Appl. Phys. **89**, 8017 (2001).

[8] J. Nitta, T. Akazaki, H. Takayanagi, and T. Enkoi, Phys. Rev. Lett. **78**, 1335 (1997).

[9] J. Luo, H. Munekata, F. F. Fang, and P. J. Stiles, Phys. Rev. B **41**, 7685 (1990).

[10] See, e.g., J. Schliemann, J. C. Egues, and D. Loss, Phys. Rev. B **67**, 085302 (2003).

[11] E. Tutuc, E. P. De Poortere, S. J. Papadakis, and M. Shayegan, Phys. Rev. Lett. **86**, 2858 (2001); S. A. Vitkalov, M. P. Sarachik, and T. M. Klapwijk, Phys. Rev. B **64**, 073101 (2001).

[12] R. Fletcher, E. Zaremba, M. D'Iorio, C. T. Foxon and, J. J. Harris, Phys. Rev. B **41**, 10649 (1990).

[13] R. Fletcher, J. J. Harris, C. T. Foxon, and R. Stoner, Phys. Rev. B

45, 6659 (1995).
[14] A. Cavalheiro, E. C. F. da Silva, E. K. Takahashi, A. A. Quivy, J. R. Leite, and E. A. Meneses, Phys. Rev. B **65**, 075320 (2002).
[15] G. Q. Hai, N. Studart, F. M. Peeters, J. T. Devreese, P. M. Koenraad, A. F. W. van der Stadt, and J. H. Wolter, in *Proceedings of the 22nd International Conference on the Phys. of Semicond.* edited by J. Lockwood (World Scientific, Singapore, 1995), p. 823.
[16] P. M. Koenraad, A. C. L. Heessels, F. A. P. Blom, J. A. A. J. Perenboom, and J. H. Wolter, Physica B **184**, 221 (1993).
[17] X. F. Wang and P. Vasilopoulos, Phys. Rev. B **67**, 085313 (2003).
[18] A. Isihara and L. Smrcka, J. Phys. C **19**, 6777 (1986).
[19] W. Xu, Appl. Phys. Lett. **82**, 724 (2003).
[20] H. C. Huang, O. Voskoboynikov, and C. P. Lee, Phys. Rev. B **67**, 195337 (2003).
[21] T. Ando, A. B. Fowler, and F. Stern, Rev. Mod. Phys. **54**, 437 (1982).
[22] G. H. Chen and M. E. Raikh, Phys. Rev. B **59**, 5090 (1999).
[23] E. G. Mishchenko and B. I. Halperin, Phys. Rev. B **68**, 045317 (2003).
[24] W. Xu, Phys. Rev. B **57**, 12939 (1998); W. Xu, I. Khmyrova, and V. Ryzhii, *ibid.* **64**, 085209 (2001).
[25] P. T. Coleridge, Phys. Rev. B **44**, 3793 (1991); P. T. Coleridge, R. Stoner, and R. Fletcher, *ibid.* **39**, 1120 (1989).
[26] C. Y. Sung, T. B. Norris, A. A. Kushaa, and G. I. Haddad, Appl. Phys. Lett. **68**, 435 (1996).